

Research

Impact resistance of macro and micro steel fibre reinforced self-compacted concrete (SFRSCC) with modelling and reliability analysis

R. Kesavamoorthi¹ · G. Mohan Ganesh¹

Received: 11 August 2023 / Accepted: 11 December 2023

Published online: 20 January 2024

© The Author(s) 2024 **OPEN**

Abstract

Adding steel fibres can transform the brittle characteristic of concrete into a ductile state. The objective of the current study is to test the impact resistance of macro and micro steel fibre-reinforced self-compacting concrete (SFRSCC) experimentally by applying a simulated drop-weight impact, as well as statistically and through reliability studies. Cube specimens were used for the experiment. The inclusion of macro and micro steel fibre greatly increased the concrete mixture's impact resistance. It is observed that the volume fraction of 0.75 and 0.50% of macro and micro steel fibre has improved impact resistance with an increase in the percentage of energy absorption of 216.21 and 240.53%, respectively. All the concrete samples exhibited the same failure pattern. Using Response Surface Methodology, the impact resistance of SFRSCC mixtures can be accurately predicted. The first and failure cracks (N1 and N2) follow a two-parameter Weibull distribution function of drop-weight impact test.

Article Highlights

- The impact resistance of self-compacting concrete reinforced with macro and micro steel fibers at volume fractions of 0.25, 0.50, 0.75, and 1%.
- The quantity of admixture increases the workability of SCC in compensation for the decrease in workability caused by the addition of steel fiber. When steel fibers are incorporated into SFRSCC, its mechanical properties are enhanced.
- In comparison to conventional SCC, the impact energy absorption of macro and micro steel fibers is enhanced. Response surface methodology enables precise prediction of the impact resistance of SFRSCC mixtures.

Keywords Macro and Micro steel fibre · Drop-weight impact test · Self-Compacting concrete · Response surface methodology · Weibull distribution

Abbreviations

SCC	Self compacting concrete
SFRSCC	Steel fiber reinforced self-compacting concrete
SEM	Scanning electron microscopy
CF	Crimped steel fiber
SCM	Supplementary cementations materials

✉ G. Mohan Ganesh, gmohanganesh@vit.ac.in | ¹School of Civil Engineering, Vellore Institute of Technology, Vellore 632014, India.



WD	Weibull distribution
N_1	First crack
N_2	Final crack
RSM	Response surface methodology
RDWI	Repeated Drop Weight Impact test
FRC	Fiber reinforced concrete
VMA	Viscosity modifying agent
SP	Superplasticizer
EFNARC	European federation of national associations representing for concrete
ACI	American concrete institute
λ	Ductility index
E_1	Initial crack impact energy
E_2	Final crack impact energy
LF	Length of fiber

1 Introduction

There is a high probability that several structures and structural components may be exposed to impact loads or constant impacts over their active life. There are a variety of impact forces, each having its own distinct origin [1]. There are several instances, including the impact of automobile crashes on building structures. Possible occurrences include dropping objects from greater heights and the impact of projectiles in conflict or terrorist activities [2]. The most typical damage to a precast concrete pile is the spalling of its head during its driving operation [3]. In some cases, a high impact velocity results in significant damage. Particularly for brittle materials such as concrete, impact forces result in fleeting dynamic loads, exposing the material to stresses it was not meant to withstand [4]. Steel and synthetic fibres have been included into concrete mixtures as a potential solution to absorb these types of pressures [5]. For instance, Fiber Reinforced Concrete (FRC) enhances impact resistance, impact energy absorption, and dynamic strength significantly. In recent years, the use of FRC in civil and military construction applications has expanded dramatically [6]. Examples of FRC applications include channel lining, bridge decks, industrial flooring, and airport pavement, offshore structures, and naval facility. Researchers have produced guidelines for evaluating FRC under impact resistance using various methodologies [7]. The tests are categorized based on the impact load mechanism and the investigated parameters. Tests include the Charpy impact test, the Repeated drop-weight test, the Steady strain-rate test, the Projectile impact test, the Split-Hopkinson bar test, the Explosive test, and the Instrumented pendulum impact test [8]. As there is limited data and different impact tests, it is tough to compare the variation in outcomes, and some are difficult to conduct and need specialist equipment [9]. The American Concrete Institute (ACI 544.2R-89) suggests assessing the impact strength of fibrous concrete with a simple Repeated Drop Weight Impact test (RDWI) [5].

In addition, the RDWI test findings are distributed, which makes it difficult to analyze the data. In a study conducted by Nataraja et al. [10], the impact resistance of FRC with 27.5 mm-long crimped steel fibre was examined. Nili and Afroughsabet [3] assessed the impact resistance of concrete reinforced with polypropylene. The use of silica fume and polypropylene fibres enhanced impact resistance, especially at a concentration of 0.5% fibres. In a separate investigation [11], the same authors substituted 60 mm in length hooked end steel fibres instead of polypropylene fibres at 0.5 and 1.0% volume. The composition of steel fibres increases impact resistance. Murali et al., [12] tested the impact resistance of FRC with crimped and hooked end steel fibres of 50 mm in length, 1 mm in equivalent diameter, and 50 aspect ratio. The result demonstrates a greater improvement in impact resistance than standard concrete. Janani and Santhi [13] examined the impact resistance of FRC using the modified RBDWI test technique with steel fibre 30 mm in length, diameter of 0.5 mm, and volume fractions of 0.75, 1.15, and 1.50 percent. The research showed that FRC has significantly greater impact resistance than normal concrete in terms of the quantity of blows.

Self-compacting concrete may be compacted by its own weight without the need for external vibration, despite having weak tensile and impact strength. These properties are enhanced by inclusion fibres [14, 15]. In addition to enhancing concrete's strength and structural performance, fibres diminish the mixture's workability. Resistance to filling, passing ability, and segregation may become more pronounced because of the addition of fibres to SCC [16]. The fibre content of SCC must be well regulated, [17]. Y. Ding et al., [18], conducted study on the impact resistance of High-Performance Self Compacting Concrete (HPSCC), which included steel rebar reinforcement and varied volume fraction of macro

fibres lengths of 30 mm and diameter of 0.67 mm. By merging steel rebars with macro fibres, the failure impact energy is enhanced up to 157 and 164% respectively. This is an effective method for increasing the impact resistance. Malavika and Chithra [19], investigated SCC hybrids reinforced with hooked end and crimped steel fibre (volume fractions of 0.25, 0.5, and 0.75%), with a diameter of 0.7 mm and a length of 70 mm. Compared with regular concrete, the inclusion of hybrid steel fibre results in a significant increase in impact resistance of 55 and 100 in the 0.75% of volume fraction. Sallal R. Abid et. al., [20] conducted a drop-weight impact test on FR-SCC. Straight micro steel fibres were added into the mixture with volume fractions of 0.5, 0.75 and 1.0%, respectively. The addition of micro steel fibre in self-compacting concrete improved the impact resistance with 114 and 243%. Micro-steel fiber-reinforced SCC with different fibre content: 0, 0.50, 0.750, and 1% subjected to flexural impact showed increase in increased impact resistance and ductility [21, 22].

The above literature study demonstrates that there is a great deal of research on FRC with impact resistance and the mechanical characteristics of SCC. However, there is a paucity of research on the drop-weight impact resistance of macro and micro steel fiber-reinforced SCC. This study focuses on the impact resistance of macro and micro steel fibre-reinforced SCC. The micro and macro steel fibre content were employed as an input variable in Response Surface Methodology (RSM) models designed to quantify the impact energy of first and failure cracks. Using the Weibull distribution and reliability analysis, impact resistance data was analyzed.

2 Research gap

It is found that assessment of impact resistance of macro and micro steel fibre reinforced self-compacting concrete using RDWI is lacking in technical literature this connection, this study aims to fill the research gap to evaluate the impact resistance of SFRSCC comparing of different fiber volume fractions.

The subsequent sections of this study are structured as follows. In the following section, the materials and testing procedures are discussed upon. The results of the SEM analysis regarding the physical and mechanical properties of SFRSCC, in addition to its impact resistance, are given in Sect. 3. In Sect. 4, the improvement of SFRSCC's impact resistance through the application of response surface methodology is discussed. An evaluation of impact resistance is provided in Sect. 5, employing the Weibull distribution and reliability analysis. Section 6 concludes this paper.

3 Materials and methods

3.1 Materials used

Concrete mixtures of SFRSCC were made with OPC (Grade 53) (IS 12269–2013) [33]. The manufactured sand was adapted as fine aggregate with a fineness modulus of 2.65 and specific gravity of 2.55. The crushed natural stone, passed through a 12.5 mm sieve and retained on a 10 mm sieve, was used in this study as per IS 383–2016 [34]. The cement and aggregates were procured from local vendors in Vellore. A polycarboxylate ether-based superplasticizer (SP) was added to the concrete mixture at a dosage of 1.7% by weight of cement to achieve the appropriate workability and 0.05% (0.28 kg/m³) of viscosity modifying agent (VMA) was used as a segregation resistance. BASF India Limited, Construction Chemicals Division, located in Kancheepuram, Chennai, supplied the admixtures. Crimped steel fibre with a diameter of 0.5 mm and lengths of 12 mm (micro) and 30 mm (macro) with an aspect ratio of 24 and 60 were used, as shown in Fig. 1. The physical properties of steel fibre include a density of 7850 kg/m³ and an ultimate tensile strength of 2850 MPa.

3.2 Sample preparation

The SCC mixtures with and without micro and macro steel fibres were manufactured in the following manner: In a concrete mixer, cement and aggregate were dry mixed for two minutes. Then water and a high-range water reducer were added and completely blended for one minute. The fibres were then mixed into the concrete mixture for three minutes [23, 24] to create a homogenous mixture. In this experimental study, nine distinct mixtures were studied. Table 1 illustrates the nine mixes of different percentages (0, 0.25, 0.5, 0.75, and 1%) of SFRSCC with two types (micro and macro) of steel fibres (by volume of concrete). The mix id is denoted as SCC V_f CF l_f . V_f is the percentage of volume fraction of steel fibre and l_f is the length of steel fibre. The mix design of SCC was developed using Nan-Su method [25]. EFNARC [26] recommended procedures such as the slump flow test, V-funnel and L Box tests were used to analyze the properties of fresh

Fig. 1 Crimped Steel Fibre

(a) Macro Fibre

(b) Micro Fibre

Table 1 Illustration of mixture proportion of Steel fibre reinforced SCC

MIX ID	Cement kg/m ³	Fine Aggregate kg/m ³	Coarse Aggregate kg/m ³	Water kg/m ³	Super Plasticizer kg/m ³	VMA kg/m ³	Weight of fibre kg/m ³	SF %
SCC0CF0	550	910	700	209	9.35	0.28	–	–
SCC0.25CF30	550	910	700	209	9.35	0.28	19	0.25
SCC0.5CF30	550	910	700	209	9.35	0.28	39	0.5
SCC0.75CF30	550	910	700	209	9.35	0.28	58	0.75
SCC1.0CF30	550	910	700	209	9.35	0.28	77	1
SCC0.25CF12	550	910	700	209	9.35	0.28	19	0.25
SCC0.5CF12	550	910	700	209	9.35	0.28	39	0.5
SCC0.75CF12	550	910	700	209	9.35	0.28	58	0.75
SCC1.0CF12	550	910	700	209	9.35	0.28	77	1

SFRSCC mix. To assess the mechanical properties of the SFRSCC mixtures, cube (100×100×100 mm) specimens were cast for drop-weight impact and compressive strength test, cylinder (Diameter—100 mm, Height—200 mm) for split tensile strength, and prisms (Size of 100×100×500 mm) for flexural strength. All specimens were demolded after 24 h and cured for 28 days before testing. The average of three specimens is used to determine each test result.

3.3 Experimental program

3.3.1 Drop-weight impact test

The approach of this investigation followed the test procedure and guidelines mentioned in Reference [13]. As shown in Fig. 2. The authors adopted the modified testing procedure, which is derived from the guidelines provided by ACI 544.2R. The size of 100 mm cubes of SFRSCC were subjected to an impact test. A hammer with 135 Newtons of mass was dropped from a height of 413 mm. A steel ball with a diameter of 64.5 mm is placed on top of the concrete cube specimen to transmit the impact load. The first crack strength (N_1), the number of blows necessary to generate the first visible fracture, and the failure strength (N_2), the number of blows needed to separate the specimen, were recorded for each specimen. The impact energy absorption of the samples during the cracking stages were determined by number of blows (N), mass of the hammer (m), and height of fall (h). Using Eq. (1) and (2), the initial and failure crack impact energy (E_1) and (E_2) absorbed by the SFRSCC specimen were computed.

$$E_1 = N_1 \cdot mgh = N_1 \frac{mv^2}{2} \quad (1)$$

$$E_2 = N_2 \cdot mgh = N_2 \frac{mv^2}{2} \quad (2)$$

where

N_1 and N_2 —Number of blows of first and failure crack.

m —Mass of the hammer in kg.

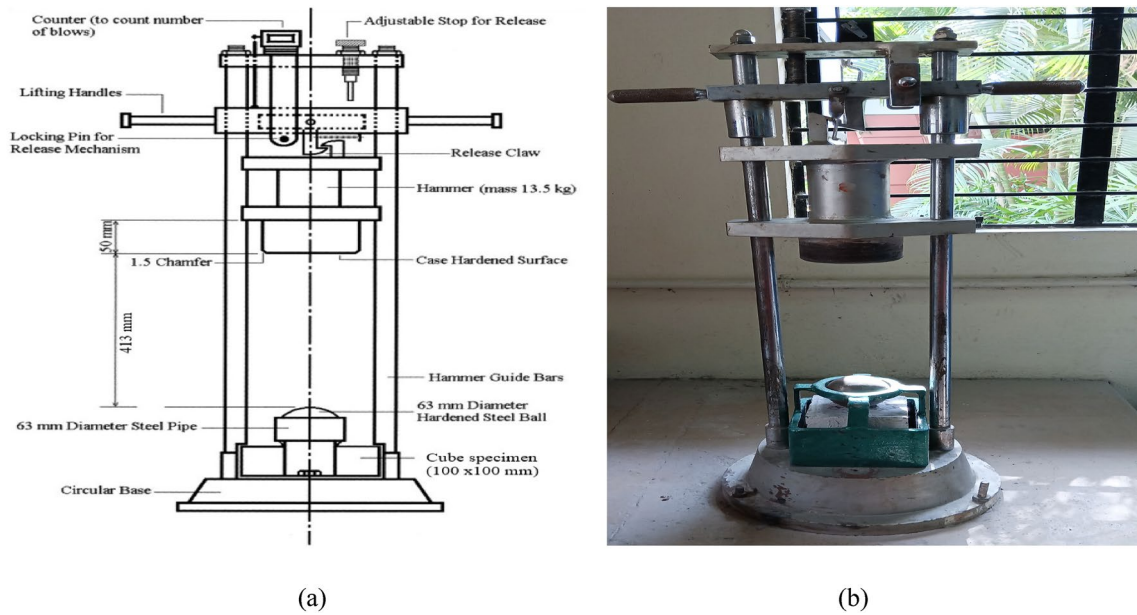


Fig. 2 Impact Test setup adopted from reference [13] **a** Schematic diagram **b** Actual test setup

h—Falling height of hammer in mm.
 g—Acceleration due to gravity in m/s.²
 v—Impact velocity in m/s.

4 Result and discussions

4.1 Results of fresh SFRSCC tests

The characteristics of fresh concrete properties such as slump flow (Flowability), V—Funnel (Filling ability) and L—Box (Passing ability) are shown in Table 2. The outcomes of slump flow, V-Funnel, and L-Box tests were compiled and compared to EFNARC requirements. The slump flows for all mixtures varied between 645 and 750 mm. The Control mixture's slump flow was greater than that of the concrete containing fibres but comparable. The V-Funnel test measures the viscosity (flow rate) of concrete, with results ranging between 3.89 and 12 s. The L-Box test on fresh concrete evaluated the capacity of the mixtures to pass past the three-bar barrier, and the presented values ranged from 0.80 to 0.84. As shown in Table 2, the test results for fibrous composites are within EFNARC's permissible limits. These findings show that the mixes have sufficient viscosity and filling capacity. Figure 3, displays a fresh concrete test experiment. Figure 3a, indicates unequivocally that the cement pastes and crimped steel fibres were combined and did not separate.

Table 2 Result on fresh properties of SFRSCC

MIX ID	SF %	Slump flow mm	EFNARC Class	V- Funnel sec	EFNARC Class	L—Box H2/H1	EFNARC Class
SCC0CF0	0	750	SF—2	3.89	VS—2	0.81	PA—2
SCC0.25CF30	0.25	730	SF—2	4.12	VS—2	0.81	PA—2
SCC0.5CF30	0.50	700	SF—2	4.92	VS—2	0.84	PA—2
SCC0.75CF30	0.75	670	SF—2	5.36	VS—2	0.81	PA—2
SCC1.0CF30	1.00	645	SF—1	5.97	VS—2	0.8	PA—2
SCC0.25CF12	0.25	710	SF—2	8	VS—2	0.81	PA—2
SCC0.5CF12	0.50	695	SF—2	10	VS—2	0.8	PA—2
SCC0.75CF12	0.75	665	SF—2	12	VS—2	0.81	PA—2
SCC1.0CF12	1.00	650	SF—1	12	VS—2	0.8	PA—2

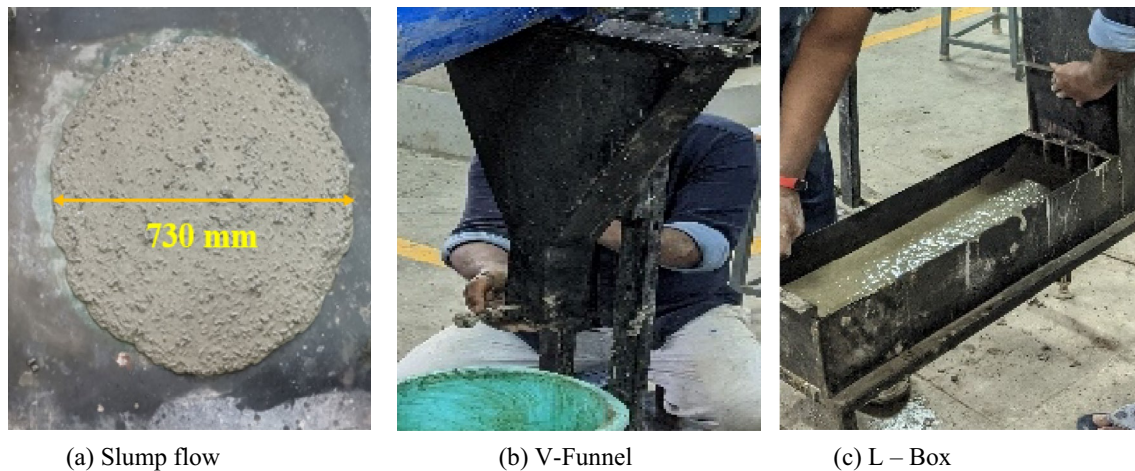


Fig. 3 Measurement of fresh Properties of steel fibre reinforced self-compacting concrete

Table 3 Result of mechanical properties of SFRSCC

Mix ID	SF in %	Compressive strength	Split tensile strength	Flexural strength
		(MPa)	(MPa)	(MPa)
		28 days	28 days	28 days
SCC0CF0	0	52.32	4.10	7.07
SCC0.25CF30	0.25	58.21	4.40	9.27
SCC0.5CF30	0.50	60.83	4.50	10.61
SCC0.75CF30	0.75	60.98	5.06	9.97
SCC1.0CF30	1.00	56.70	4.20	9.95
SCC0.25CF12	0.25	54.03	4.23	9.34
SCC0.5CF12	0.50	60.13	4.61	9.48
SCC0.75CF12	0.75	58.10	4.55	9.33
SCC1.0CF12	1.00	55.76	3.98	8.69

4.2 Results of mechanical properties

Three samples were averaged to establish the result for each mix. 108 samples were cast and analyzed to determine the compressive, split tensile, flexural, and impact resistance. The experiments were conducted according to IS 516–2021 [35] and ACI 544.2R [5].

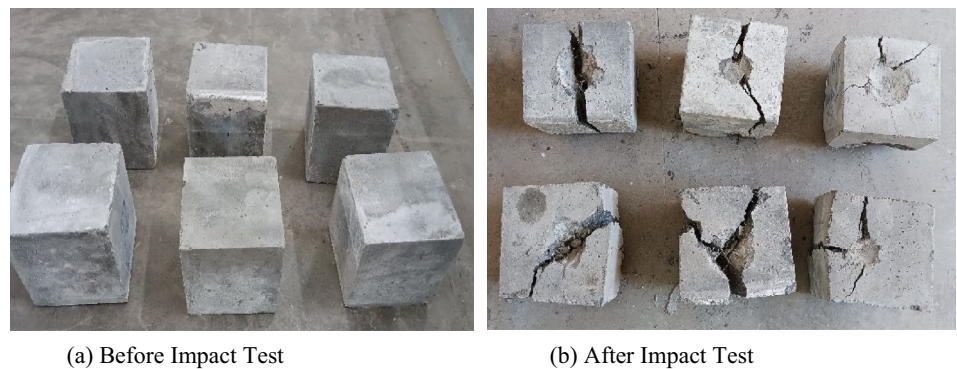
4.2.1 Result of compressive, split tensile and flexural strength

The mechanical properties of SFRSCC were evaluated according to the Indian standards, as presented in Table 3. In this experiment, it was established that the minimum compressive strength of steel fiber-reinforced SCC mixtures was around 50 MPa. The addition of macro and micro fibres to the mix increased its compressive strength compared to the control mix shown in the table.

The compressive strength of the control mixture is 52.32 MPa. The addition of macro fibre in the conventional concrete mixture enhances the compressive strength from 8.37 to 16.55%. For micro fibre compressive strength increases from 3.2 to 14.93% respectively. The compressive strength of macro fibre was found to be the highest at 0.75%, whereas micro fibre exhibited the highest strength at 0.5%. Nevertheless, it is important to highlight that all the samples of SFRSCC successfully surpassed the desired strength threshold of 50 MPa. In addition, the split tensile and flexural strengths are shown in Table 3. In comparison to previous mixes, the split tensile strength is enhanced by increasing the ratio of macro and micro fibres to 0.5 and 0.75%, respectively. The macro fibre volume fractions

Table 4 Result of impact test on SFRSCC

MIX ID	First crack N_1 (Blows)	Failure N_2 (Blows)	Ductility index ($N_2 - N_1$)/ N_1	E_1 First crack impact energy (kN mm)	E_2 Failure impact energy (kN mm)	Compressive strength (MPa)
SCC0CF0	9	12	0.32	519.80	686.88	52.32
SCC0.25CF30	14	26	0.86	779.70	1448.01	58.21
SCC0.5CF30	26	35	0.35	1448.01	1949.25	60.83
SCC0.75CF30	28	39	0.39	1559.40	2172.02	60.98
SCC1.0CF30	17	27	0.54	965.34	1485.14	56.70
SCC0.25CF12	23	38	0.65	1280.94	2116.33	54.03
SCC0.5CF12	27	42	0.56	1503.71	2339.10	60.13
SCC0.75CF12	23	34	0.48	1280.94	1893.56	58.10
SCC1.0CF12	10	23	1.30	556.93	1280.94	55.76

Fig. 4 Impact Test on SFRSCC

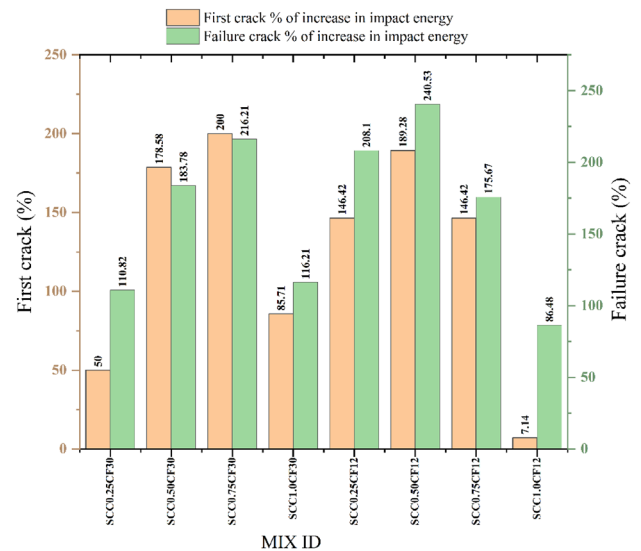
with the greatest flexural strength were 0.5%. The 0.5% volume fraction has exhibited the greatest performance in both macro and micro fibres.

4.2.2 Result of drop-weight impact test

Table 4 presents the impact resistance outcomes of SFRSCC with respect to the volumetric content of macro and micro steel fibres. The number of blows recorded during the first crack (N_1) and failure crack (N_2) are converted into absorbed impact energy (E_1 and E_2) using Eqs. (1) and (2). Figure 4, illustrates the cube specimens before and after towards the impact test.

For the control mixture, the impact energy of first crack and failure crack were measured at 519.80 and 688.8 kN mm. Figure 5, illustrates the percentage of an increase in the impact energy of SFRSCC. The inclusion of macro steel fibres, with a volume percentage ranging from 0.25 to 1.0%, led to a substantial increase in the impact energy at first crack, ranging from 50 to 200%. Similarly, the failure crack impact energy absorption ranging from 110.82 to 216.21% was observed. Adding micro steel fibres into the concrete increased the first crack impact energy absorption range from 7.14 to 189.28%. The first crack impact energy absorption with a volume fraction of 0.25–0.75% from 146.43 to 189.29%, but with a volume fraction of 1% increased it by just 7.15%. Similarly, the failure crack impact energy absorption ranging from 86.48 to 240.53% was observed. Comparing both macro and micro fibres with different volume fractions, 0.75 and 0.50% exhibit the highest failure impact energy. Because the length of the fiber and volume fraction played a significant role in it. The findings indicate that inclusion of macro and micro steel fibres in the concrete mixture enhanced the impact energy absorption. Because fibres have a better ability to absorb impact energy, the fibre concentration improved the impact resistance of concrete. Steel fibres actively bridging the fracture during the load transfer and these fibres account for a high rate of impact energy absorption.

Fig. 5 Percentage of increase in Impact energy of SFRSCC



4.2.3 Ductility index

The ductility index is used to determine the toughness of SFRSCC specimens after cracking. Ductility index is defined as the ratio of the number of cracking blows from the first crack to the final failure crack ($N_2 - N_1$) to the number of cracking blows at the first fracture (N_1).

$$\text{Ductility index}(\lambda) = \frac{(N_2 - N_1)}{N_1} \quad (3)$$

Ductility index Table 4 values demonstrate the ability of a concrete specimen to absorb impact energy. The ductility index values of SCC with addition of fibres are greater than those of SCC without added fibres. The addition of 0.25% macro and micro fibres increased the ductility index significantly, while further additions of 0.5% and 0.75 percent macro and micro fibres with SCC decreased the ductility index relative to the first addition. The ductility index of the SCC with both macro and micro fibre additions of 1% has increased significantly. The variations occurred due to the volume fraction of fibres and the agglomeration of fibres within the concrete matrix [36]. The inclusion of steel fibres in the concrete matrix converts the brittle to ductile nature of SCC.

4.2.4 Failure pattern

The conventional concrete without fibres fails suddenly, but the SFRSCC mixtures showed different failure patterns, as shown in Fig. 6. The SFRSCC specimen failed when subjected to impact testing and the development of the first crack can be seen in Fig. 6a. With the continuation of blows, the crack was developed further, and the specimen split into two parts as shown in Fig. 6b. A steel ball hits the top of the specimen, creating a circular fractured zone. Continuous loading causes diagonal stresses across the specimen, which lead to the major and lateral crack failures shown in Fig. 6c. The inclusion of steel fibres prevents the expansion of cracks and acts as a bridging between the elements, as shown in Fig. 6d. Based on these figures, the inclusion of fibres delays the failure of concrete specimens because it converts the brittle concrete into ductile.

4.2.5 SEM analysis of SFRSCC

Using scanning electron microscopy (SEM) images has helped to understand the interaction between fibres and the concrete matrix. The SEM images were acquired from the fracture surfaces of the specimens. Figure 7a, illustrates the random distribution of fibres within the concrete matrix. Figure 7b, exhibits indications of partial debonding occurring between the fibre and concrete matrix. These indications include the observation of hydrated cement products and the presence of deep scratches

Fig. 6 Failure patterns of SFRSCC under impact—**a** First crack (SCC0.5CF12) **b** Failure crack (SCC0.5CF12) **c** Fractured zone, Major failure, Lateral failure crack (SCC0.50CF30) **d** Fibres bridging crack (SCC0.25CF12)

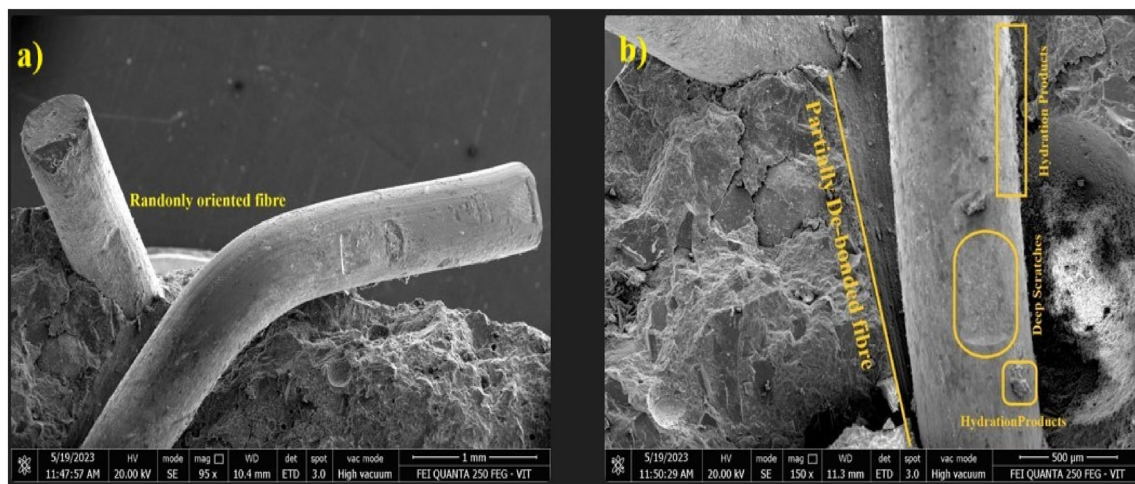
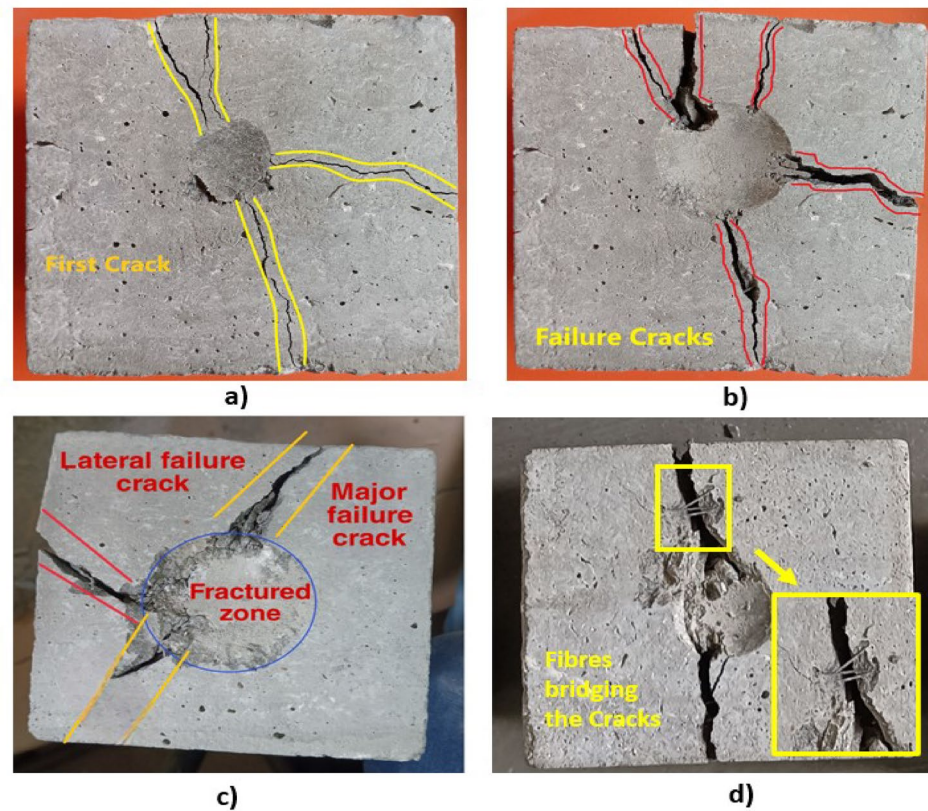


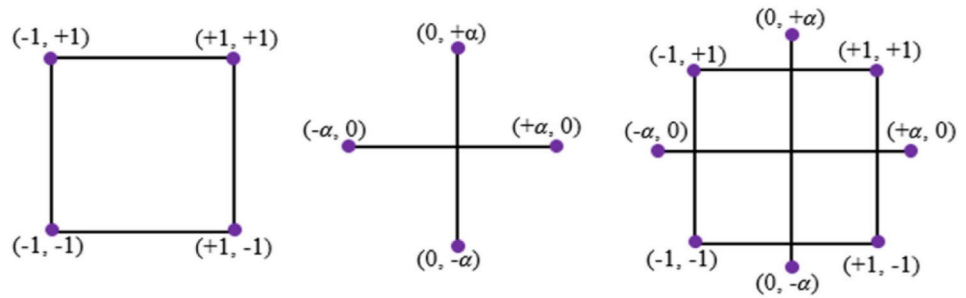
Fig. 7 SEM images of SFRSCC

on the surface of the fibre. Based on the analysis of the SEM images, it can be inferred that the interfacial bond between the fibre and concrete matrix shows a notable degree of interaction, resulting in an enhanced ability to absorb energy.

5 Response surface methodology

Response surface methodology (RSM) is widely used due to its factorial design. Star points improve the estimation of model terms in variable space by increasing the center points. It makes the fundamental design model more flexible. Figure 8, depicts the CCD framework, which is comprised of four factorial points (1) and (α). The CCD model was used to forecast the impact

Fig. 8 Central composite design (CCD) framework [27]



resistance of eight mixtures with three levels of the variable (Macro and Micro steel fibres) distance between the design center and axial run. $\alpha=1$ was chosen. The Eq. (4) and (5) assess the response of the model with both linear and nonlinear independent variables [27, 28].

$$y = \gamma_0 + \gamma_1 C_1 + \gamma_2 C_2 + \dots \dots \gamma_n C_n + \epsilon \tag{4}$$

where y is response of the model, γ_0 —intercept of y , $C_1=C_2=0$, γ_1 —the coefficient of the first independent variable, γ_2 —the coefficient of the second independent variable, C_1 and C_2 are variable coefficient, and ϵ is the error. The Eq. (5) demonstrates that the dataset and a higher-degree polynomial model are not linear.

$$y = \gamma_0 + \sum_{i=1}^k \gamma_i C_i + \sum_{i=1}^k \gamma_{ii} C_i^2 + \sum_{i < j} \gamma_{ij} C_i C_j + \epsilon \tag{5}$$

In which, y is response of the model, C_i and C_j are coded values of input variables, i —the linear coefficient, j —the quadratic coefficient, γ —the regression constant, γ_0 —the y -intercept for $C_i=C_j=0$, k is the number of variables, and ϵ is the error. The RSM model used to simulate variables and responses is shown in Table 5. ANOVA’s assessment of the model’s significance and performance is shown in Table 6.

The RSM/CCD model of quadratic response variations is shown in Table 6 with ANOVA results. The established models were all statistically significant, with p -values of 0.004% for the E_1 and 0.024% for the E_2 , using F -values of 50.40 and 15.33 for the first crack (E_1) and failure crack (E_2) impact energy, respectively. The significance and terms of the created models were assessed with 95% confidence (i.e., p 0.05). In the initial crack impact energy model, the length of fibre (LF) terms with p -values of 0.546 are insignificant. The failure impact energy model terms SF, SF * SF, and SF*LF likewise obtained significant p -values, whereas the model term LF had a p value of 0.206. Figure 10 illustrates a 3D surface map of both the first and failure impact energies. Predicted model equations for actual responses are shown in Eq. (6) and (7). Model terms with a minus or plus sign preceding them indicate independent variables having an antagonistic or synergistic influence on responses.

$$E_{1pre} = 862 + 3748 * SF - 40.74 * LF - 4418 * SF^2 + 68.07SF * LF \tag{6}$$

Table 5 The RSM model response of SFRSCC mixtures

Mix ID	Variables		Responses	
	SF (%)	Length (mm)	First crack impact energy (kN mm)	Failure impact energy (kN mm)
SCC0.25CF12	0.25	12	1280.94	2116.33
SCC0.25CF30	0.25	30	779.70	1448.01
SCC0.5CF12	0.5	12	1503.71	2339.10
SCC0.5CF30	0.5	30	1448.01	1949.25
SCC0.75CF12	0.75	12	1280.94	1893.56
SCC0.75CF30	0.75	30	1559.40	2172.02
SCC1.0CF12	1	12	556.93	1280.94
SCC1.0CF30	1	30	965.34	1485.14

Table 6 Analysis of variance result for SFRSCC model

Response	Variable	Sum of squares	Df	Mean square	F-value	p-value	Significant
First crack impact energy	Model	921238	4	230310	50.4	0.004	Yes
	SF	74819	1	74519	16.31	0.027	Yes
	LF	2110	1	2110	0.46	0.546	No
	SF*Sf	610043	1	610043	133.51	0.001	Yes
	SF*LF	234566	1	234566	51.34	0.006	Yes
Failure crack impact energy	Model	994438	4	248610	15.33	0.024	Yes
	SF	171289	1	171289	10.7	0.047	Yes
	LF	41401	1	41401	2.59	0.206	No
	SF*Sf	511824	1	811824	31.97	0.011	Yes
	SF*LF	269924	1	269924	16.86	0.026	Yes

$$E_{2pre} = 2024 + 3002 * SF - 53.6 * LF - 4047 * SF^2 + 73.01SF * LF \quad (7)$$

E_1 indicates the impact energy of the first fracture, E_2 represents the impact energy of failure (in kN mm), SF represents the volume percentage of the fibre (in%), and LF represents the length of the fibre (in mm). As indicated in Table 7, In this research RSM models were used to assess the prediction performance using statistical parameters, which may quantify a model's capacity to transmit goodness-of-fit criteria. The statistical criteria that are shown in Table 8 indicate that the developed models have a sufficient level of accuracy. Figure 9. illustrates the association between the actual and predicted response models using scatter plots. The projected response of first crack and failure energy using E_1 model with $R^2 = 0.9892$ and E_2 model with $R^2 = 0.9736$ was accurate despite considering all the elements that contributed to their prediction accuracy. Figure 10. illustrates the 3D plot of first and failure impact energy.

6 Analysis of weibull distribution on impact resistance of SFRSCC

Weibull Distribution (WD), which is used often in engineering applications. This statistical method analyses dependability using shape and scale variables. According to previous studies, two-parameter Weibull distributions are superior for assessing the concrete's impact resistance and fatigue. By presenting an increasing or decreasing danger function, WD determines structural behaviour. The drop-weight impact test data was analyzed using the two-parameter WD function. Since fatigue and drop-weight tests involve repetitive loads, the probability function $F(N)$ of the drop-weight impact test is given by Eq. (8) [29]

Table 7 Verification of statistical parameters and model

Response	R^2	Adj. R^2	Pred. R^2	Mean	SD	COV (%)	AP
First crack impact energy	0.99	0.97	0.75	1172	365	31	43.23
Failure impact energy	0.95	0.89	0.55	1836	386	21	97.07

Table 8 Result on impact resistance of SFRSCC of actual and predicted values

Mix ID	E_1 First crack impact energy (kNmm)	E_{1pre} First crack impact energy (kNmm)	% Diff	E_2 Failure impact energy (kNmm)	E_{2pre} Failure impact energy (kNmm)	% Diff
SCC0.25CF12	1280.94	1238.22	3.33	2116.33	2097.36	0.90
SCC0.25CF30	779.70	811.21	-4.04	1448.01	1461.06	-0.90
SCC0.5CF12	1503.71	1551.04	-3.15	2339.10	2308.5	1.31
SCC0.5CF30	1448.01	1430.35	1.22	1949.25	2000.25	-2.62
SCC0.75CF12	1280.94	1311.62	-2.40	1893.56	2012.86	-6.30
SCC0.75CF30	1559.40	1497.25	3.99	2172.02	2033.56	6.37
SCC1.0CF12	556.93	519.96	6.64	1280.94	1211.81	5.40
SCC1.0CF30	965.34	1011.90	-4.82	1485.14	1561.01	-5.11

Fig. 9 Scatter Plot Actual and Predicted of First (E_1) and Failure (E_2) Impact energy

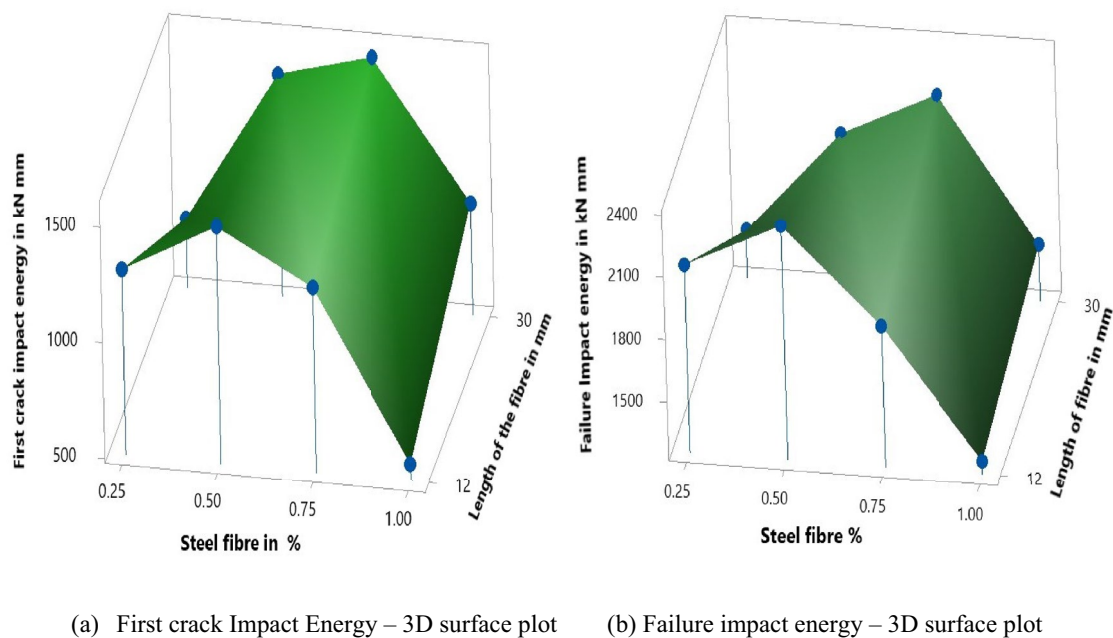
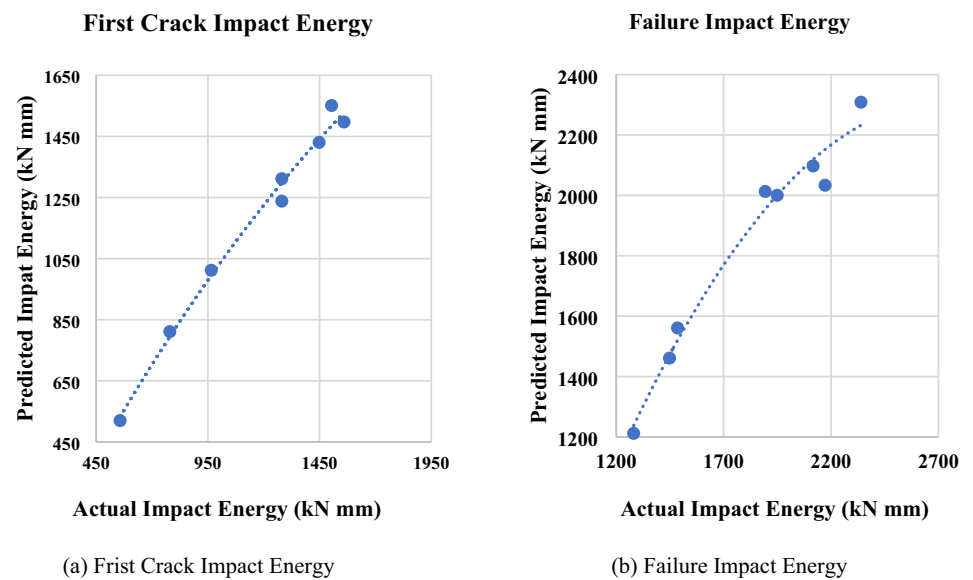


Fig. 10 3D surface plot of Impact energy

$$F(N) = \frac{\gamma}{Z - a_0} \left[\frac{a - a_0}{Z - a_0} \right]^{\gamma-1} * Exp \left\{ - \left[\frac{a - a_0}{Z - a_0} \right]^\gamma \right\} \quad Z \leq a \leq \infty \tag{8}$$

Equation (9) is produced by integrating Eq. (8) with the random variable distribution function $F(N_r)$.

$$F(N_r) = p(N \leq N_r) = 1 - Exp \left\{ - \left[\frac{a - a_0}{Z - a_0} \right]^\gamma \right\} \tag{9}$$

where n —random variable N , γ —shape parameter, Z —scale factor, and a_0 location parameter. The drop weight impact test assumes a minimum concrete life of zero. As a result, Eq. (10) gives the survival probability function $F(N_r)$.

$$F(N_r) = 1 - \text{Exp} \left\{ - \left[\frac{a - a_o}{Z - a_o} \right]^\gamma \right\} \quad (10)$$

Taking natural logarithm twice of Eq. (10) and re-arranging it yields Eq. (11)

$$\ln \left\{ \ln \left[\frac{1}{F(N_r)} \right] \right\} = \gamma \ln(n) - \gamma \ln(Z) \quad (11)$$

The Eq. (11) assesses results of the SFRSCC drop-weight impact test conform to the two-parameter WD function. Equation (11) solved as a linear and comparing it to a straight-line ($y = ax + b$) generates γ , $\gamma \ln(z)$, and R^2 . The formula for $F(N_r)$ as shown in Eq. (12) [30].

$$F(N_r) = Q_k = 1 - \frac{M}{J + 1} \quad (12)$$

where M —failure or increasing order of number of blows and J —total number of concrete mixes.

The two-parameter Weibull probability distribution of the drop-weight impact test result where $\ln(1/Q_k)$ and $\ln(n)$ are linear. Table 9 demonstrates that $\ln(1/Q_k)$ correlates with $\ln(\ln(N_1))$ and $\ln(N_2)$, and Fig. 11, displays the appropriate values for these variables. The regression coefficients γ , $\gamma \ln z$, and (R^2) for the number of blows N_1 and N_2 are shown in Table 10. For the impact resistance result of mixtures, the linear expression between $\ln(\ln(1/Q_k))$ and \ln has R^2 values larger than 0.85. (N_1, N_2). Thus, the Weibull distribution may be utilized to measure SFRSCC impact resistance, and it is also referenced in the studies [31].

7 Reliability analysis

The findings of the SFRSCC impact test follow a two-parameter Weibull probability distribution, according to a study of the Weibull distribution. The WD would be used to assess the cracking blows based on the impact test results of SFRSCC mixes. Calculate the SFRSCC specimen failure probability (P') using Eq. (13) In reliability analysis, the scale and the shape factor are important parameters that help to describe the underlying probability distribution and predicts the failure of the specimen or the duration it will withstand. Probability distributions used in estimating reliability, such as the Weibull distribution, often associate these factors [32].

$$N = y \left\{ \ln(1 - P')^{(1/\gamma)} \right\} \quad (13)$$

where N is the number of blows, P' is failure probability, y —scale factor, and γ —shape factor. The survival probability η of SFRSCC specimens can be estimated using Eq. (14)

$$\eta = 1 - P' \quad (14)$$

The survival probability of the design number of the first crack and the failure crack resulting from impact blows on SFRSCC specimens is given in Table 11. Figure 12, indicates the survival probability of the first and failure fracture strength of the SFRSCC. The SFRSCC specimens should be crack-resistant over their entire service life. With an 80% chance of

Table 9 Analysis Weibull distribution of SFRSCC

MIX ID	First crack N_1	Failure crack N_2	Rank	$Q_k = 1 - (M / (J + 1))$	$\ln(1/Q_k)$	$\ln(\ln(1/Q_k))$	$\ln(N_1)$	$\ln(N_2)$
OSCC0SF	9	12	1	0.9	0.11	-2.25	2.20	2.48
SCC1.0CF12	10	23	2	0.8	0.22	-1.50	2.30	3.14
SCC0.25CF30	14	26	3	0.7	0.36	-1.03	2.64	3.26
SCC1.0CF30	17	27	4	0.6	0.51	-0.67	2.83	3.30
SCC0.75CF12	23	34	5	0.5	0.69	-0.37	3.14	3.53
SCC0.25CF12	23	38	6	0.4	0.92	-0.09	3.14	3.64
SCC0.50CF30	26	35	7	0.3	1.20	0.19	3.26	3.56
SCC0.50CF12	27	42	8	0.2	1.61	0.48	3.30	3.74
SCC0.75CF30	28	39	9	0.1	2.30	0.83	3.33	3.66

Fig. 11 Weibull distribution plot

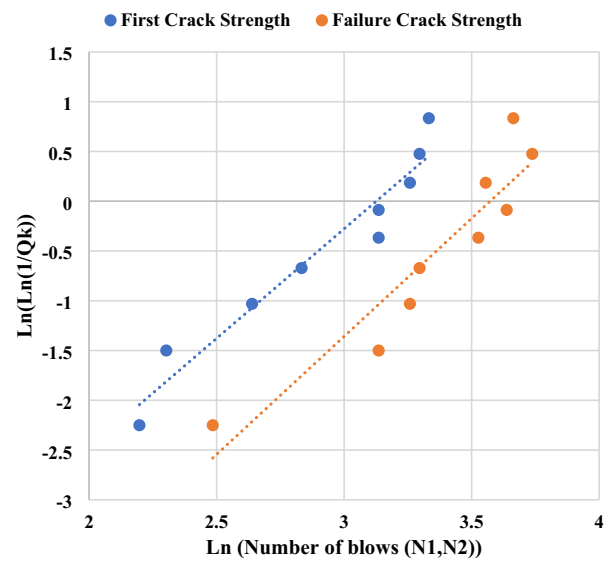


Table 10 Regression analysis of Weibull distribution

Impact resistance	Regression coefficient γ (Shape factor)	Regression coefficient $\gamma \ln(z)$	Characteristic life (z)	R^2
First crack strength (N_1)	2.20	6.87	23	0.9394
Failure strength (N_2)	2.37	8.47	36	0.8751

Table 11 Survival probability of impact resistance of SFRSCC

Impact resistance	$\eta=0.01$	$\eta=0.2$	$\eta=0.6$	$\eta=0.8$	$\eta=0.99$
First crack strength	46	29	17	12	3
Failure strength	69	44	27	19	5

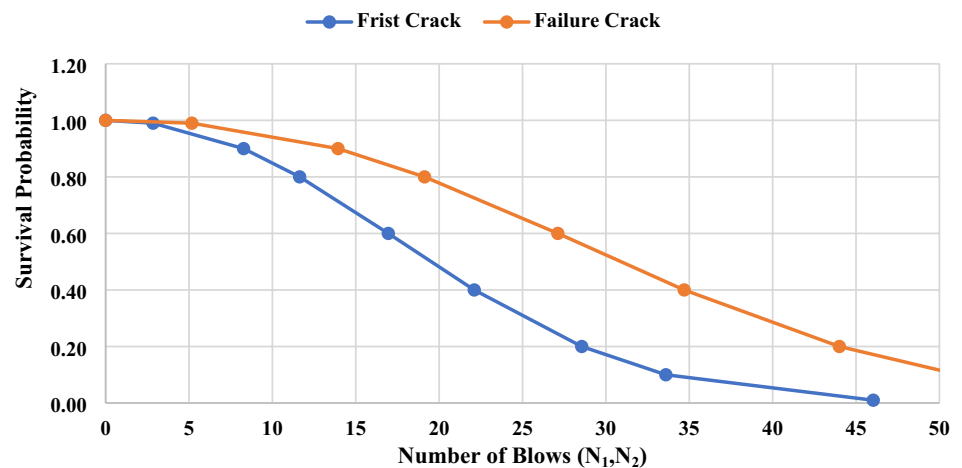
survival and a 20% possibility of failure. The design cracking blows at the first crack and failure crack are, respectively, 12 and 19. It indicates that 80% of SFRSCC specimens can withstand these blows.

8 Conclusions

The impact resistance of Macro and Micro reinforced SCC mixtures was assessed using RWDI test. The following findings were reached after performing RSM, Weibull distribution, and reliability analyses on the drop-weight impact test results:

- The incorporation of macro and micro fibres significantly improved the impact resistance of SFRSCC concrete specimens.
- Due to the inclusion of macro fibres with volume fractions of 0.5 and 0.75 percent, the impact blow retention of specimens at first crack (N_1) and failure (N_2) is enhanced.
- Similarly, micro fibres exposed to impact resistance with volume fractions of 0.25 and 0.50% demonstrate many improved outcomes on first fracture (N_1) and failure load (N_2).
- The bridging effect of macro fiber in concrete is superior compared to micro fiber. Steel fibers addition to conventional concrete to improve both its ability to bridge cracks and its ability to absorb impact energy.
- With R^2 values of 0.98 (E_1) and 0.97 (E_2) for SFRSCC, the response surface method demonstrated the strong agreement between the variables and responses.
- The failure pattern of SFRSCC is observed better than the conventional SCC. Both the inclusion of micro and macro steel fibres delays the failure of concrete specimens because it converts the concrete brittle into ductile.

Fig. 12 Plot of reliability probability for impact resistance of SFRSCC



- Cube specimens adhere to the two-parameter WD function, and the macro and micro steel fibres of the first and failure crack impact energy of SFRSCC. According to the findings of the reliability investigation, about 80% of the concrete sample could sustain 12 blows during the first crack stage and 19 blows during the failure strength stage.

For engineering field applications such as highway and dam building, the fire resistance, durability, corrosion of steel fibres and SCM replacement might be investigated extensively.

Acknowledgements The authors feel highly indebted to chancellor of Vellore Institute of Technology, Vellore, Tamil Nadu, India for providing the opportunity to pursue our research.

Author contributions KR Experimental work, formal analysis, Investigation, Writing—original draft. GMG Conceptualization, Methodology, Supervision.

Funding The authors declare that this study did not receive any funding in any form.

Data availability The data collected from an experimental laboratory work based on request it can be provided; data is available based on request.

Declarations

Competing interests The authors declare that they have no known competing financial interests or personal relationships that could have appeared to influence the work reported in this paper.

Open Access This article is licensed under a Creative Commons Attribution 4.0 International License, which permits use, sharing, adaptation, distribution and reproduction in any medium or format, as long as you give appropriate credit to the original author(s) and the source, provide a link to the Creative Commons licence, and indicate if changes were made. The images or other third party material in this article are included in the article's Creative Commons licence, unless indicated otherwise in a credit line to the material. If material is not included in the article's Creative Commons licence and your intended use is not permitted by statutory regulation or exceeds the permitted use, you will need to obtain permission directly from the copyright holder. To view a copy of this licence, visit <http://creativecommons.org/licenses/by/4.0/>.

References

1. Naik TR. Sustainability of concrete construction. *Pract Period Struct Des Constr.* 2008;13:98–10. [https://doi.org/10.1061/\(asce\)1084-0680\(2008\)13:2\(98\)](https://doi.org/10.1061/(asce)1084-0680(2008)13:2(98)).
2. Bentur SM. Introduction. *Fibre Reinf Cem Compos.* 2020. <https://doi.org/10.1201/9781482267747-8>.
3. Nili M, Afroughsabet V. Combined effect of silica fume and steel fibers on the impact resistance and mechanical properties of concrete. *Int J Impact Eng.* 2010;37:879–86. <https://doi.org/10.1016/j.ijimpeng.2010.03.004>.
4. Zhang MH, Li L, Paramasivam P. Flexural toughness and impact resistance of steel-fibre-reinforced lightweight concrete. *Mag Concr Res.* 2004;56:251–62. <https://doi.org/10.1680/macr.2004.56.5.251>.
5. ACI Committee 544, Shah SP. Measurement of properties of fiber reinforced concrete. *ACI Mater J.* 1988;85:583–93. <https://doi.org/10.14359/2355>.

6. Zhu XC, Zhu H, Li HR. Drop-weight impact test on U-shape concrete specimens with statistical and regression analyses. *Materials*. 2015;8:5877–90. <https://doi.org/10.3390/ma8095281>.
7. Badr AF, Ashour AK, Platten. Statistical variations in impact resistance of polypropylene fibre-reinforced concrete. *Int J Impact Eng*. 2006;32:1907–20. <https://doi.org/10.1016/j.ijimpeng.2005.05.003>.
8. Yoo DY, Banthia N. Impact resistance of fiber-reinforced concrete—A review. *Cem Concr Compos*. 2019;104: 103389. <https://doi.org/10.1016/j.cemconcomp.2019.103389>.
9. Abid SR, Abdul Hussein ML, Ali SH, Kazem AF. Suggested modified testing techniques to the ACI 544-R repeated drop-weight impact test. *Constr Build Mater*. 2020;244: 118321. <https://doi.org/10.1016/j.conbuildmat.2020.118321>.
10. Nataraja MC, Dhang N, Gupta AP. Statistical variations in impact resistance of steel fiber-reinforced concrete subjected to drop weight test. *Cem Concr Res*. 1999;29:989–95. [https://doi.org/10.1016/S0008-8846\(99\)00052-6](https://doi.org/10.1016/S0008-8846(99)00052-6).
11. Nili M, Afroughsabet V. The effects of silica fume and polypropylene fibers on the impact resistance and mechanical properties of concrete. *Constr Build Mater*. 2010;24:927–33. <https://doi.org/10.1016/j.conbuildmat.2009.11.025>.
12. Murali G, Santhi AS, Mohan Ganesh G. Impact resistance and strength reliability of fiber reinforced concrete using two parameter weibull distribution. *J Eng Appl Sci*. 2014;9(4):554–9. <https://doi.org/10.14716/ijtech.v5i2.403>.
13. Janani S, Santhi AS. Multiple linear regression model to predict mechanical properties of hooked-end steel fibre-reinforced blended concrete. *Int J Technol*. 2019;49(3):526–36. <https://doi.org/10.14716/ijtech.v9i3.763>.
14. Okamura H, Ouchi M. Self-compacting concrete. *J Adv Concr Technol*. 2003;1:5–15. <https://doi.org/10.3151/jact.1.5>.
15. Nanthagopalan P, Santhanam M. Fresh and hardened properties of self-compacting concrete produced with manufactured sand. *Cem Concr Compos*. 2011;33:353–8. <https://doi.org/10.1016/j.cemconcomp.2010.11.005>.
16. Aydin AC. Self compactability of high volume hybrid fiber reinforced concrete. *Constr Build Mater*. 2007;21:1149–54. <https://doi.org/10.1016/j.conbuildmat.2006.11.017>.
17. Uysal M, Yilmaz K. Effect of mineral admixtures on properties of self-compacting concrete. *Cem Concr Compos*. 2011;33:771–6. <https://doi.org/10.1016/j.cemconcomp.2011.04.005>.
18. Ding Y, Li D, Zhang Y, Azevedo C. Experimental investigation on the composite effect of steel rebars and macro fibers on the impact behavior of high performance self-compacting concrete. *Constr Build Mater*. 2017;136:495–505. <https://doi.org/10.1016/j.conbuildmat.2017.01.073>.
19. Mahakavi P, Chithra R. Impact resistance, microstructures and digital image processing on self-compacting concrete with hooked end and crimped steel fiber. *Constr Build Mater*. 2019;220:651–66. <https://doi.org/10.1016/j.conbuildmat.2019.06.001>.
20. Nuruddin MF, Chang KY, Azmee NM. Workability and compressive strength of ductile self compacting concrete (DSCC) with various cement replacement materials. *Constr Build Mater*. 2014;55:153–7. <https://doi.org/10.1016/j.conbuildmat.2013.12.094>.
21. Mezzal SK, Al-Azzawi Z, Najim KB. Effect of discarded steel fibers on impact resistance, flexural toughness and fracture energy of high-strength self-compacting concrete exposed to elevated temperatures. *Fire Saf J*. 2020;121:103271. <https://doi.org/10.1016/j.firesaf.2020.103271>.
22. Athiyamaan G V. Mohan Ganesh, “Analysis of the alignment of micro-steel fibers in admixture- based self-compacting concrete (MSFR-SCC) using NDT and evaluation of its effect on the modulus of rupture.” *Int J Technol*. 2019;10(1):5–15. <https://doi.org/10.14716/ijtech.v10i1.2066>.
23. Nataraja MC, Nagaraj TS, Basavaraja SB. Reproportioning of steel fibre reinforced concrete mixes and their impact resistance. *Cem Concr Res*. 2005;35:2350–9. <https://doi.org/10.1016/j.cemconres.2005.06.011>.
24. Danish P, Ganesh GM. Durability properties of self-compacting concrete using different mineral powders additions in ternary blends. *Revista Romana de Mater/Roman J Mater*. 2020;50(3):369–78.
25. Su N, Hsu KC, Chai HW. A simple mix design method for self-compacting concrete. *Cem Concr Res*. 2001;31:1799–807. [https://doi.org/10.1016/S0008-8846\(01\)00566-X](https://doi.org/10.1016/S0008-8846(01)00566-X).
26. EFNARC (2005) The European Guidelines for Self-Compacting Concrete. The European Guidelines for Self-Compacting Concrete 63.
27. Haruna SI, Zhu H, Shao J. Experimental study, modeling, and reliability analysis of impact resistance of micro steel fiber-reinforced concrete modified with nano silica. *Struct Concr*. 2022. <https://doi.org/10.1002/suco.202100651>.
28. Athiyamaan V, Ganesh GM. Statistical and detailed analysis on fiber reinforced self-compacting concrete containing admixtures - a state of art of review. *IOP Conf Series Mater Sci Eng*. 2017. <https://doi.org/10.1088/1757-899X/263/3/032037>.
29. Murali G, Santhi AS, Ganesh GM. Impact resistance and strength reliability of fiber reinforced concrete using two parameter weibull distribution. *Int J Technol*. 2014;2:111–20. <https://doi.org/10.1416/ijtech.v5i2.403>.
30. Murali G, Gayathri R, Ramkumar VR, Karthikeyan K. Two statistical scrutinize of impact strength and strength reliability of steel Fibre-Reinforced Concrete. *KSCE J Civil Eng*. 2018;22:257–69. <https://doi.org/10.1007/s12205-017-1554-1>.
31. Rahmani T, Kiani B, Shekarchi M, Safari A. Statistical and experimental analysis on the behavior of fiber reinforced concretes subjected to drop weight test. *Constr Build Mater*. 2012;37:360–9. <https://doi.org/10.1016/j.conbuildmat.2012.07.068>.
32. Abid SR, Abdul-Hussein ML, Ayoob NS, Ali SH, Kadhun AL. Repeated drop-weight impact tests on self-compacting concrete reinforced with micro-steel fiber. *Heliyon*. 2020;6:e03198. <https://doi.org/10.1016/j.heliyon.2020.e03198>.
33. B. of Indian Standards, “IS 12269. (2013). Ordinary Portland Cement. 53 Grade — Specification”.
34. B. of Indian Standards, “IS 383. (1970). Sp.cification for coarse and fine aggregates.
35. B. of Indian Standards, “IS 516- 1. (2021). Hardened Concrete – Methods of Test. Part 1: Testing of Strength of Hardened Concrete”.
36. Abid SR, et al. Impact performance of steel fiber -reinforced self-compacting concrete against repeated drop weight impact. *Crystals* vol 1. 2021;11(2):1–17. <https://doi.org/10.3390/cryst11020091>.